

Article

Characteristics of Zinc Adsorption onto Biochars Derived from Different Feedstocks

Jiajia Liu ^{1,*}, Fei Wang ² and Wangqi Xu ²¹ Environmental Engineering College, Nanjing Polytechnic Institute, Nanjing 210044, China² Institute of Geotechnical Engineering, School of Transportation, Southeast University, Nanjing 210096, China

* Correspondence: antileliujiajia@163.com

Abstract: Human activities such as the discharge of urban sewage, garbage, and industrial waste have seriously affected the quality of groundwater sources for human consumption. The potential for using biochar as a reactive medium in a permeable reactive barrier (PRB) was explored for Zn-contaminated groundwater treatment in this study. Four different types of biochar produced from wood, coconut shell, rice straw, and fruit shell were used. The production temperature of these biochars were 600 °C, 550 °C, 500 °C, and 500 °C, respectively. The samples were coded with the initials of the biochar source and the production temperature as WD600, CS550, RS500, and FS500. The results of various batch adsorption studies show that equilibrium solution pH has a great effect on the maximum adsorption capacity in the pH range of 2–7. The adsorption of Zn on biochars follows the Freundlich model and fits well with the pseudo-second-order model. The fixed-bed column test data were well fitted to the Dose–Response model. The adsorption capacities of WD600, CS550, RS500, and FS500 were 24.91, 15.87, 9.25, and 46.71 mg/g, respectively. The removal rate of FS500 can reach a maximum of 98.87%. FS500 is considered to be a potential reaction medium for treating Zn-contaminated groundwater in a PRB system. This work provides a new option for converting biomass waste into an adsorbent for zinc in wastewater. The results of this study are expected to provide a solid theoretical basis for the further application of biochar in groundwater pollution remediation.

Keywords: permeable reactive barrier; adsorption; biochar; zinc; kinetic



Citation: Liu, J.; Wang, F.; Xu, W. Characteristics of Zinc Adsorption onto Biochars Derived from Different Feedstocks. *Water* **2023**, *15*, 3789. <https://doi.org/10.3390/w15213789>

Academic Editors: Tianxiang Wang and Alex Neumann

Received: 26 September 2023

Revised: 26 October 2023

Accepted: 26 October 2023

Published: 29 October 2023



Copyright: © 2023 by the authors. Licensee MDPI, Basel, Switzerland. This article is an open access article distributed under the terms and conditions of the Creative Commons Attribution (CC BY) license (<https://creativecommons.org/licenses/by/4.0/>).

1. Introduction

As a precious water resource, groundwater not only provides a significant amount of drinking water for human beings but also supports agricultural planting and industrial production. However, the discharge of urban sewage, garbage, and industrial waste, as well as runoff from the intensive use of fertilizer and pesticides, have resulted in serious environmental problems. China's ecological environment status bulletin (MEP, 2017) reported that the percentages of monitoring wells with poor water quality and extremely poor water quality were 45.4% and 14.7%, respectively [1]. With the release of the Law on the Prevention and Control of Soil Pollution of the People's Republic of China (NPC, 2018) and the Water Pollution Control Action Plan (The State Council, 2015), there is a strong drive by the Chinese government for each department to integrate scientific and technological resources, to speed up the research of common key technologies, such as soil and groundwater pollution remediation and pollution control, treatment, and remediation through relevant, well-funded national science and technology projects and to develop advanced equipment and efficient and low-cost functional materials [2,3].

In recent years, the groundwater in China has been polluted by heavy metals to varying degrees. The zinc content of groundwater in some areas has seriously exceeded the national standard, which has posed a serious threat to the health of local residents. However, there are few studies on the treatment methods of groundwater with excess

zinc contents. It is meaningful to study the treatment of zinc-contaminated groundwater since, in some areas, only the groundwater can be used for drinking [4]. The World Health Organization (WHO) and the United States Environmental Protection Agency (USEPA) set the permissible limit for zinc(II) in drinking water as 5 mg/L. The Department of Environment (DOE) in Malaysia set the permissible limit for zinc(II) in drinking water as 3 mg/L. In China, the limit is 1 mg/L according to the GB/T 14848-2017 Groundwater Quality Standard [5].

There are many methods to remove zinc in water. Chemical methods include coagulation, precipitation, sulfide, and precipitation. However, the disadvantages are also obvious, like cost, difficulties of large-scale application, and probability of secondary pollution [6,7]. Physical methods include the use of membranes, ion exchange, and adsorption (by activated carbon, minerals, or biochar). All of these methods have good prospects for removing heavy metals in groundwater, but relevant studies are limited [8,9]. The low-cost preparation and regeneration technology of activated carbon still needs continuous research and development and has better application prospects.

The adsorption properties of biochar for heavy metals are mainly affected by biomass type, pyrolysis temperature, solution pH, and heavy metal type and concentration. Chen studied the adsorption properties of Zn(II) in solution by biochar using hardwood (HW450) pyrolysis at 450 °C and corn stalk pyrolysis at 600 °C (CS600) [10]. It was found that the removal rate increased with the pH and reached a maximum value at 6.5. The adsorption effect of CS600 on Zn(II) in the solution was significantly better than that of HW450. Li used water hyacinth prepared at 200–500 °C to study its adsorption of zinc in aqueous solution [11]. The results showed that biochar prepared at 500 °C had the strongest adsorption capacity, and its adsorption mechanism was mainly the complexation between functional groups in biochar and metal ions. The adsorption process of zinc by biochar can be described by a quasi-second-order model ($R^2 > 0.95$). The adsorption experiment results showed that wheat straw carbon prepared at low temperature has a strong adsorption capacity of Zn(II) under acidic conditions. The researchers have carried out a lot of research work on biomass types, preparation conditions, and the mechanism of biochar adsorption of heavy metals [12]. Due to the wide variety of biomass, the preparation conditions of biochar also have a great influence on its physicochemical properties, heavy metal adsorption mechanism, and kinetic process. Therefore, it is necessary to further study the physicochemical properties of biochar and its adsorption properties and kinetics of heavy metals.

The permeable reactive barrier (PRB) is a promising sustainable remediation technique invented in the early 1990s that has drawn great attention in recent years [13–16]. The use of sustainable reactive media is one of the key components of PRBs, the type of which depends on the target contaminants, their concentration, the mechanisms needed for their removal, and the hydro-geological site conditions [13,17–19]. Biochar, which has been studied extensively worldwide, is a sustainable sorbent for the heavy-metal remediation of water and soil [20]. The introduction of biochar enabled the use of inexpensive filling materials to enhance the effectiveness of PRBs. The application of biochar in PRB requires a good understanding of many factors, including the adsorption characteristics of contaminants onto biochar, the reaction speed of various contaminants with biochar, and the physical and chemical reactions involved in the complex wall system [21,22]. However, research on the application of biochar as the reactive material in PRBs is limited. Kumar et al. assessed the U(VI) removal rate of switchgrass biochar from groundwater. They claimed that the sorption capacity of switchgrass biochar was approximately 2.12 mg of U g⁻¹ of biochar [23]. The pH of the system is a key factor in the adsorption process. Their results indicate that biochar could be used as an effective reactive barrier medium for U(VI)-contaminated groundwater. Gillham and O'Hannesin used zero-valent iron to degrade halogenated aliphatics and found that the adsorption rate constant is linked to the surface area-to-volume ratio, whereas the degradation rates are independent of velocity [24]. They also proposed in situ and aboveground applications for the remediation of contaminated groundwater. Beiyun et al. studied risk mitigation by waste-based (including wood-derived

biochar) PRBs for groundwater pollution control at e-waste recycling sites [25]. The results show that waste-based PRBs are a technically feasible and economical way to mitigate human health risks through the proper selection of adsorbents. However, these limited studies did not focus on the most commonly used biochars in the Chinese market, and there is a lack of research on the related adsorption and desorption characteristics.

The properties of biochar, such as specific surface area, pH, and surface chemistry, are highly dependent on the feedstock of biochar and the pyrolysis conditions [26,27]. Hence, the effectiveness of different biochars in treating polluted groundwater is varied [28]. Shen et al. investigated the sorption of lead by biochar produced from British broadleaf hardwood; the results show that the biochar particle size and the initial solution pH have a significant impact on lead sorption [20]. Shen et al. used biochars produced from wheat straw pellets and rice husk at 550 and 700 °C to study the adsorption characteristics and mechanisms of Ni²⁺ on these biochars [29]. The results show that the adsorption capacities of Ni²⁺ for the wheat straw pellet biochar performed better than the rice husk biochar, and a higher production temperature at 700 °C contributed a better sorption compared to that at 550 °C. In addition, although the study of Tan et al. found that rice straw biochar was the most effective in decreasing Cd enrichment in rice plants compared to bran and husk biochars, limited studies have investigated the adsorption characteristics or mechanisms of Zn²⁺ on biochars [30].

Accordingly, this study compares the adsorption characteristics of zinc from groundwater onto biochars produced from wood at 600 °C, coconut shell at 550 °C, rice straw at 500 °C, and fruit shell at 500 °C and explores the potential application of biochar in the PRB system for groundwater remediation. The detailed objectives were (1) investigating the adsorption characteristics of Zn²⁺ on these four biochars; (2) estimating the influence of groundwater conditions such as the initial groundwater pH and the initial concentration of Zn²⁺ on the adsorption capacity of biochars; and (3) analyzing the adsorption kinetics of Zn²⁺ on these four kinds of biochars.

2. Material and Methods

2.1. Biochar

Biochar powders derived from wood, coconut shell, rice straw, and fruit shell were purchased from the Liyang Desheng activated carbon plant. The production temperatures of these biochars were 600 °C, 550 °C, 500 °C, and 500 °C, respectively. The samples were coded with the initials of the biochar source and the production temperature as WD600, CS550, RS500, and FS500. The physicochemical properties of the biochars are shown in Table 1. The properties, such as surface area, particle size, ferric salts, mass density, and moisture content, were obtained from the supplier. The particle sizes of WD600, CS550, RS500, and FS500 are >0.075 mm, >0.075 mm, 0.075–0.15 mm, and 0.09–0.18 mm, respectively. The pH values of the biochars were determined in the laboratory according to the GBT 12496.7 [31]. The cation exchange capacity (CEC) of biochar was tested through a compulsive exchange method, which can be found in Gillman and Sumpter [32]. Zinc nitrate hexahydrate, sodium nitrate, nitric acid, sodium hydroxide, and barium chloride dihydrate were obtained from the Chengdu Kelon chemical reagent plant. The chemicals of Zn(NO₃)₂·6H₂O, NaNO₃, HNO₃, NaOH, and BaCl₂·2H₂O used in this study were AR-grade.

Table 1. The physicochemical properties of the biochars.

	WD600	CS550	RS500	FS500
Surface area (m ² /g)	>700	>900	>300	>500
pH	8.98	6.89	3.49	10.84
CEC (cmol/kg)	6.86	5.54	4.30	7.31
Particle size (mm)	>0.075	>0.075	0.075–0.15	0.09–0.18
Ferric salts (%)	<0.1	<0.05	<0.1	<0.1
Mass density (mg/L)	<450	<450	<450	<500
Moisture content (%)	<10	<10	<10	<10

2.2. Batch Adsorption Studies

2.2.1. Kinetic Study

Batch kinetic experiments were performed at pH 7, and an initial Zn^{2+} concentration of 50 mg/L was used to estimate the equilibrium time for the adsorption reaction. A solution of 50 mg/L Zn^{2+} in 0.01 M $NaNO_3$ was prepared, after which 0.1 g of biochar (WD600, CS550, RS500, or FS500) was added to 20 mL of the $Zn(NO_3)_2$ solution. The mixture was shaken at 200 rpm and 25 °C. The reaction time was set at 5 min, 10 min, 20 min, 30 min, 1 h, 2 h, 3 h, 6 h, 12 h, or 24 h. At the end of the experiment, aqueous samples were filtered through 0.22 μm filters, acidified, and analyzed by a Thermo Scientific spectrometer (ICE3300).

2.2.2. Equilibrium Study

The initial concentrations of the Zn^{2+} solutions used in these experiments were varied at 10, 30, 60, 80, 100, 200, and 300 mg/L, and the experiment was conducted in a 0.1 M $NaNO_3$ solution. The pH of these Zn^{2+} solutions was adjusted to 5. After this preparation, 0.1 g of biochar (WD600, CS550, RS500, or FS500) was then added to 20 mL of the $Zn(NO_3)_2$ solution. The mixtures were shaken for about 24 h at 25 °C. At the end of the specified time, the aqueous samples were filtered, acidified, and analyzed as described above.

2.2.3. Effect of pH

The pH-related adsorption study was observed by studying the Zn^{2+} adsorption in a solution of 50 mg/L Zn^{2+} in 0.01 M $NaNO_3$ over a pH range of 2–7. The pH of each initial solution was adjusted to 2, 3, 4, 5, 6, and 7 by solutions of 0.01–1 M $NaOH$ or HNO_3 . Then, 0.1 g of biochar (WD600, CS550, RS500, or FS500) was added to 20 mL of 50 mg/L $Zn(NO_3)_2$ solutions in 0.1 M $NaNO_3$. The mixtures were placed in a constant-temperature incubator shaker (25 °C) and were shaken at 200 rpm for 24 h to reach equilibrium. After filtration of the samples through a 0.22 μm filter, the equilibrium pH of each solution was measured by a pH meter. The concentration remaining in the solution was then measured by atomic absorption spectrometry after dilution and acidification. The concentration of Zn^{2+} was measured by a Thermo Scientific spectrometer (ICE3300). All tests in this study were performed in triplicate. The procedural blanks were run in parallel to eliminate possible adsorption of Zn^{2+} on tubes and filters.

2.3. Fixed-Bed Column Study

To simulate the application of biochars in removing Zn^{2+} from aqueous solutions, fixed-bed column experiments were conducted in an acrylic cylinder with a height of 200 mm and an internal diameter of 26 mm. The biochars WD600 and RS500 were mixed uniformly with sand and packed in the column to yield the desired 100 mm bed length. The ratios of biochars to the sand applied in the column were 1:9 and 2:8, respectively. The $Zn(NO_3)_2$ solution, with an initial concentration of 50 mg/L, was pumped downwards at a constant flow rate of 1 mL/min through a peristaltic pump (BT 100S). The liquid was collected from the bottom outlet every 10 min and then filtered with 0.45 μm filters before the measurement of Zn^{2+} concentration.

3. Results and Discussion

3.1. Kinetics

Because the adsorption of Zn^{2+} by RS500 and FS500 was rapid, the initial phase, in which the equilibrium constant Q_e usually increases with time, was not observed. Hence, the kinetic data were not considered to be suitable for further analysis using the kinetic model. Therefore, the results of only the WD600 and CS550 kinetics studies were fitted in this paper using the pseudo-first-order model and pseudo-second-order model to study their adsorption mechanism (Figures 1 and 2). Correlation coefficient (R^2) and Akaike information criterion (AIC) values were used to find a better-fitting model. The AIC is based on the concept of entropy and can evaluate the complexity of the estimated model

and the goodness of the fit. A model with a higher correlation coefficient and a lower AIC value is preferred. The pseudo-second-order equation fitted the data better, with higher regression coefficients of WD600 and CS500 at 0.83 and 0.73 and lower AIC values than the counterparts obtained from the pseudo-first-order model (Table 2). The calculated q_e of WD600 and CS500 were 8.19 mg/g and 6.44 mg/g, whereas the experimental q_e were 9.656 mg/g and 6.885 mg/g, respectively. The well-fitted data indicate that the dominant adsorption mechanism of Zn on WD600 and CS500 is chemisorption [20,33]. All these data indicate that the pseudo-second-order model is preferred for the adsorption kinetics of Zn on biochars; this agrees well with the studies of Shen et al. [20,29].

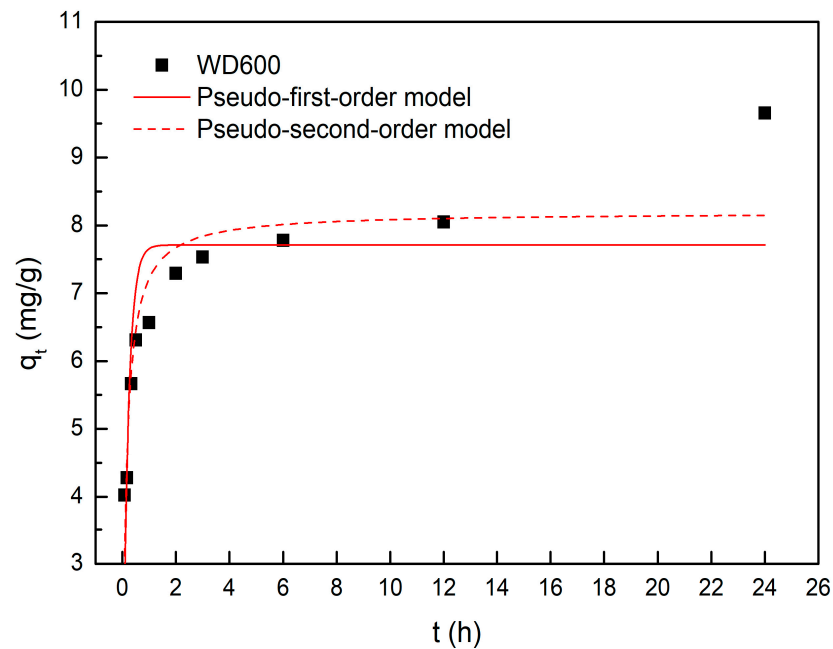


Figure 1. The fitting of pseudo-first-order and pseudo-second-order models for Zn adsorption onto WD600.

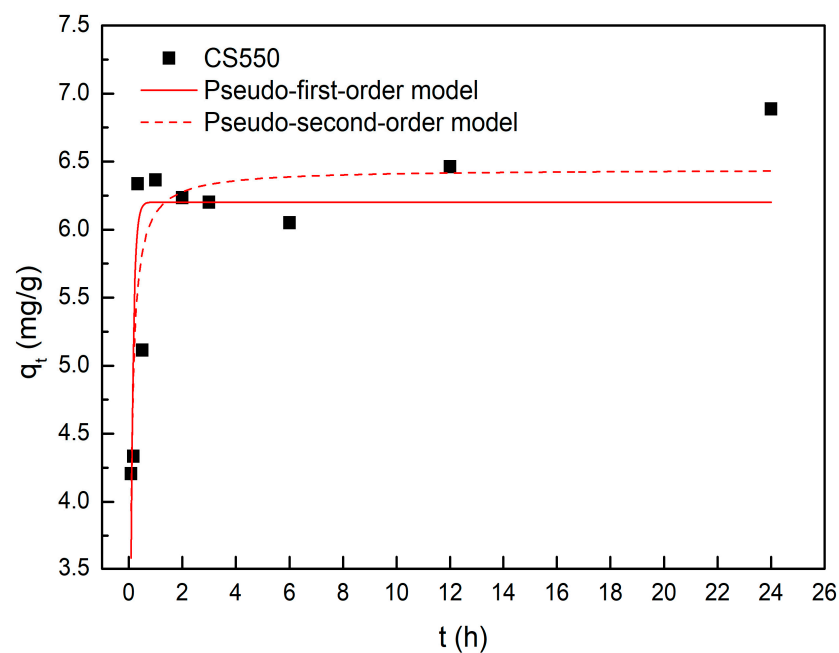


Figure 2. The fitting of pseudo-first-order and pseudo-second-order models for Zn adsorption onto CS500.

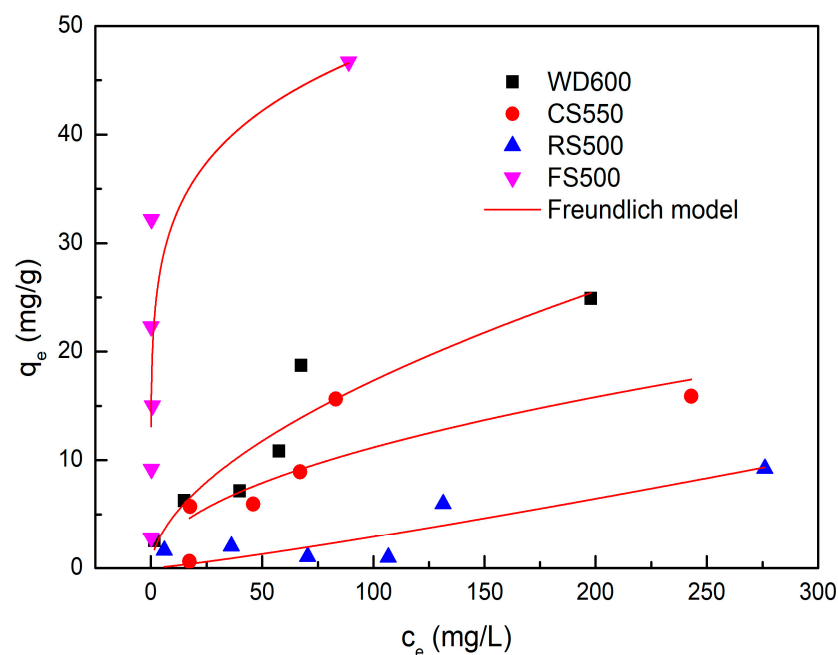
Table 2. Adsorption kinetics fitting results of WD600 and CS550.

Biochar	Pseudo-First-Order Model				Pseudo-Second-Order Model			
	k_1 (1/h)	q_e (mg/g)	R^2	AIC	K_2 (g/mg/h)	q_e (mg/g)	R^2	AIC
WD600	4.94 ± 1.24	7.71 ± 0.41	0.66	8.01	0.89 ± 0.24	8.19 ± 0.33	0.83	0.61
CS550	10.30 ± 2.19	6.20 ± 0.22	0.60	-2.81	2.92 ± 0.86	6.44 ± 0.21	0.73	-6.63

The adsorption of Zn^{2+} onto FS500, CS550, and RS500 reached equilibrium within 5 min. However, it took more than 30 min for WD600 to reach equilibrium. Although the adsorption amount was accumulated over time, the adsorption speed was reduced over the same time period. This may be due to the distribution of the initial abundance of unsaturated positions on the surface of biochars. The highest adsorption capacities of WD600, CS550, RS500, and FS500 tested in this kinetic study were 9.656 mg/g, 6.885 mg/g, 2.615 mg/g, and 15.390 mg/g, respectively. The equilibrium times of RS500 and FS500 were consistent with the results of Shen et al. [19], in which an equilibrium was reached in 5 min using biochars derived from mixed softwood and Miscanthus straw to adsorb Ni. Smaller particle sizes of biochar were found to aid the mass transport of adsorbate inside the adsorbent [34].

3.2. Adsorption Isotherms

Figure 3 shows the influence of initial Zn^{2+} concentrations (10–300 mg/L) on the adsorption amount of 0.1 g biochar. The adsorption amount of each biochar clearly increases with the increase in initial Zn^{2+} concentrations from 10 mg/L to 200 mg/L. The Zn^{2+} adsorption amount of biochar in a 300 mg/L initial Zn^{2+} solution was found to be lower than that of a 200 mg/L initial Zn^{2+} solution. This decrease in Zn adsorption follows the decrease in net negative surface charge density, although this decrease could also be partially due to a limited number of adsorption sites [35]. Indeed, at low Zn levels, the biochars were unsaturated with respect to Zn. However, with the increase in Zn^{2+} concentration, competition between cations for adsorption sites and electrostatic repulsion have a marked effect on the adsorption of Zn.

**Figure 3.** Isotherm plots for Zn^{2+} adsorption onto biochars.

Among the four biochars, the adsorption and removal of Zn in FS500 was 2–5 times higher under various initial Zn^{2+} concentrations than in the other three biochars. The highest Zn adsorption by FS500 was 46.71 mg/g. Meanwhile, the highest Zn adsorption amount by RS500 was only 9.25 mg/g. At adsorption equilibrium, the order of the amount of Zn adsorption of the four biochars was FS500 > WD600 > CS550 > RS500. This agrees well with the order of the percentage of Zn removal of biochars under a pH range of 2–7.

Based on the equilibrium adsorption of Zn on biochars, the experimental data were fitted using isotherm models, including the Langmuir, Freundlich, Sips, and BET models. Except for the Freundlich model, the other models did not match the experimental data, so they were not provided in Figure 3. For the Freundlich model, K_F is the adsorption capacity of the adsorbent (mg/g); $1/n$ ranges between 0 and 1 and is a measure of the adsorption intensity or surface heterogeneity, and the surface of the adsorbent is more heterogeneous if its value is closer to zero. As can be found from Table 3, R^2 values of WD600, CS550, RS500, and FS500 for the Freundlich model were 0.868, 0.642, 0.719, and 0.516, respectively. The R^2 values of FS500 were extremely low. In the Freundlich model, as K_F is the adsorption capacity of the adsorbent, the larger the K_F value, the stronger the adsorption capacity of that biochar. The results show that the order of K_F of the four biochars is FS500 > WD600 > CS550 > RS500. The $1/n$ values of WD600, CS550, RS500, and FS500 were 0.56, 0.50, 1.15, and 0.17, respectively, which indicates that the surface of FS500 is more heterogeneous compared to the other biochars used in this study.

Table 3. Precipitation isothermal parameters of Zn^{2+} adsorption in WD600, CS550, RS500, and FS500.

	Freundlich Isotherm Mode		
	K_F (L/mg)	$1/n$	R^2
WD600	1.32 ± 0.76	0.56 ± 0.12	0.868
CS550	1.11 ± 0.96	0.50 ± 0.18	0.642
RS500	0.01 ± 0.03	1.15 ± 0.38	0.719
FS500	21.5 ± 5.07	0.17 ± 0.06	0.516

3.3. Influence of Initial Solution pH on Zn^{2+} Adsorption

The significant effect of the initial and equilibrium solution pH's on the sorption of Zn^{2+} on biochars is shown in Figure 4, which shows that Zn^{2+} will precipitate to form $Zn(OH)_2$ when the solution pH is at 7.94 [36]. When the solution pH is higher than 8, zinc complex compounds are produced [36–38]. At pH 9–12, $Zn(OH)_2$ was considered to be the controlling phase [36]. Hence, a pH range of 2–7 was selected in this study.

As can be seen in Table 1, the pH values of WD600, CS550, RS500, and FS500 are 8.98, 6.89, 3.49, and 10.84, respectively. The high pH of FS500 at 10.84 did not significantly increase the equilibrium solution pH of 3.07 when the initial solution pH was 2 (Figure 4). However, when the initial solution pH was 3, the equilibrium solution pH values of WD600, CS550, and FS500 were increased significantly to 6.87, 5.65, and 10.28, respectively. In other words, despite the low pH of RS500 at 3.49, the equilibrium solution pH values of WD600, CS550, and FS500 were increased in various degrees with the addition of biochars. A similar increase in the equilibrium solution pH after adding biochars was found at initial solution pHs of 4–7. The equilibrium solution pH was found to be the highest (7.71%, 6.69%, 4.32%, and 10.7% for WD600, CS550, RS500, and FS500, respectively) when the initial pH was 7. However, no matter what type of biochar (except RS500) was used in this study, an insignificant increase in equilibrium solution pH values at initial pHs of 3–7 was noticed in Figure 4. This resistance to pH change may be because of the buffering capacity of biochar. Because the pH of RS500 is 3.49, the equilibrium solution pH was raised to 3.2 when the initial pH was 3, and the equilibrium solution pH was lowered to 4.32 when the initial pH was 7.

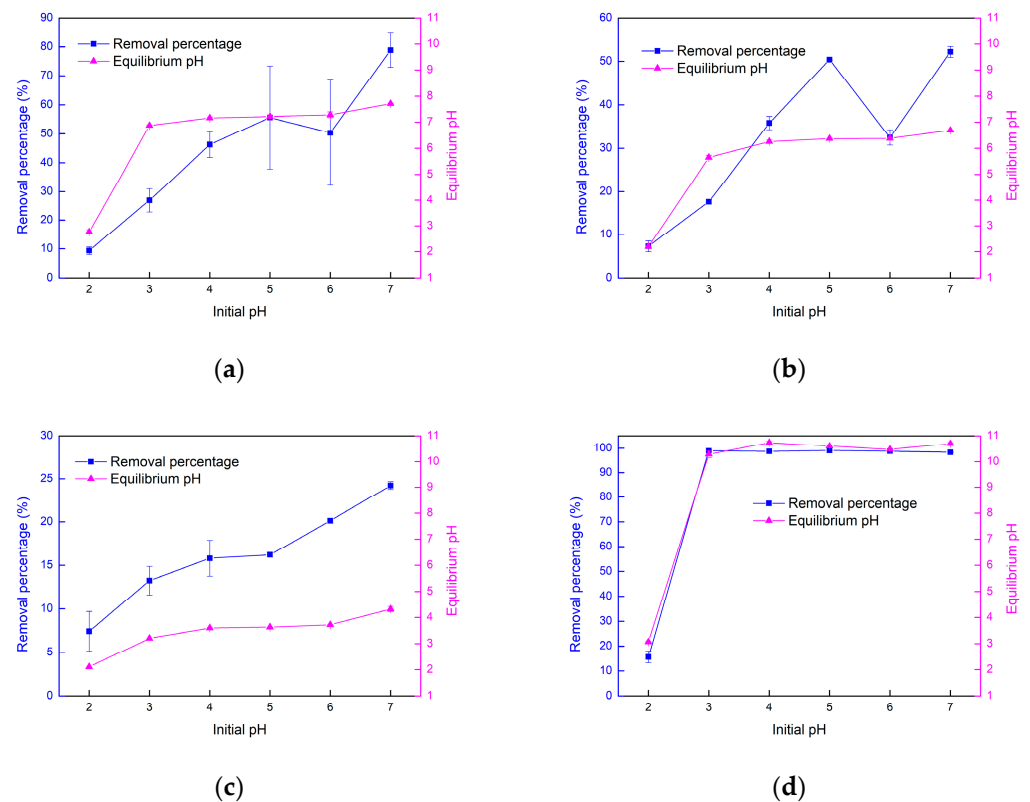


Figure 4. The influence of initial solution pH on the Zn²⁺ removal percentage of (a) WD600, (b) CS550, (c) RS500, and (d) FS500.

The adsorbent surface charge and the dissociation or protonation of organic weak electrolytes are determined by their equilibrium solution pH values [36,39]. At pH 2, the surface of the biochars was dominated by positively charged points. As a result of this electrostatic repulsion between positively charged ions on the biochar surface and Zn²⁺ in solution, the Zn²⁺ removal percentages using the four biochars were the lowest at the lowest pH (9.34%, 7.23%, 7.42%, and 15.65% for WD600, CS550, RS500, and FS500, respectively). This observation agrees well with the proposal of Wang and Al-Tabbaa that due to the physical adsorption of Zn on particle surfaces or its chemical fixation as a Zn complex, an extensive portion of Zn is dissolved when the solution pH is 2. At pH 3, these values were increased to 24.33%, 17.09%, and 13.24% for WD600, CS550, and RS500, respectively [37]. The increase in the Zn²⁺ removal rate of FS500 was even more significant, from 15.64% to 98.87%. The Zn²⁺ removal percentages of FS500 remained nearly constant within initial pH values of 3–7 because of the buffering capacity of the biochar [19]. One reason for the slow growth of Zn²⁺ removal percentages at initial pH 2–7 for RS500 was likely due to electrostatic repulsion with Zn²⁺ under an acidic environment. The Zn²⁺ removal rates of WD600 and CS550 at initial pH 6 were decreased. This observation agrees well with the proposal of Feng [40]. The solution's initial pH value significantly influenced the adsorption, and the optimum pH value for Zn(II) was 6.0. Each heavy metal ion has a limiting pH, and when the solution pH exceeds its limiting pH, the metal ion will exist in other forms and produce precipitation. Masoumeh et al. studied biochars from apple wood (WB) and rice straw (RB) and found that Zn adsorption increasing the initial pH of solutions from 4 to 6 increased the Zn adsorption in RB600, RB300, and WB600 [41]. These results indicate the high efficiency of FS500 in treating Zn-contaminated liquids when the pH is higher than 3 and the potential application of FS500 in PRB systems.

3.4. Column Test

Fixed-bed column studies were significant in simulating the practical application of adsorbents in treating contaminated water and in assessing their viability and feasibility. The Dose-Response model, the Thomas model, and the Yoon-Nelson model were applied to fit the experimental data and to predict breakthrough curves in Figures 5 and 6. The mass of adsorbents was determined, and the column kinetic parameters obtained from the models are presented in Table 4, in which a , K_{Th} , K_{YN} are the constants of the corresponding models, q_0 is the maximum concentration of solute in the solid phase, R^2 is the correlation coefficient, and T_b is the breakthrough time ($C/C_0 = 0.5$) predicted by the Yoon-Nelson model. Due to the higher values of R^2 , the Dose-Response model is better fitted to the data than the other models are.

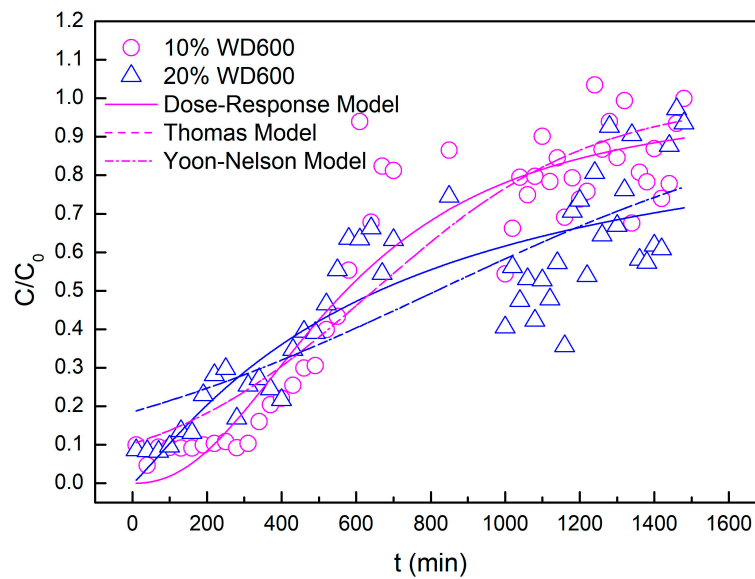


Figure 5. Experimental data and mathematical model fitting of the adsorption of Zn^{2+} to WD600.

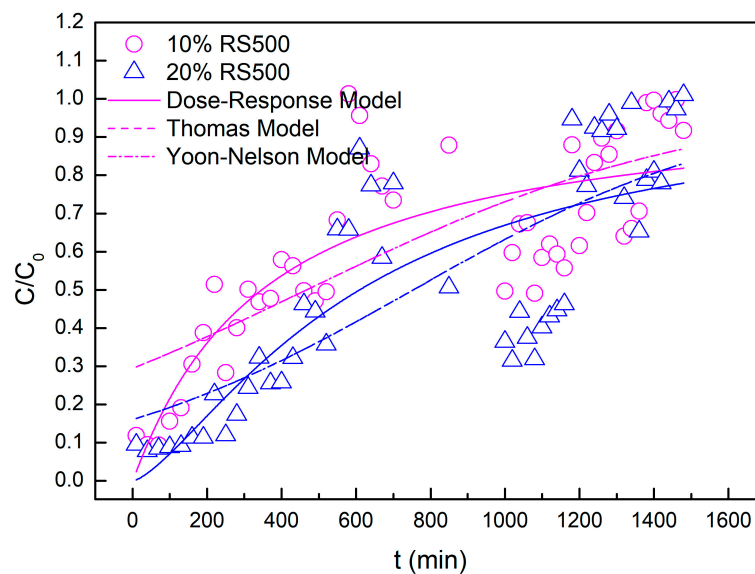


Figure 6. Experimental data and mathematical model fitting of the adsorption of Zn^{2+} to RS500.

Table 4. Mathematical model parameters for the adsorption of Zn^{2+} to the biochars.

		10% WD600	20% WD600	10% RS500	20% RS500
Mass of Adsorbents (g)		2.13	4.36	3.80	7.22
Model	Parameters				
Dose-Response	a	2.27 ± 0.22	1.14 ± 0.14	1.04 ± 0.14	1.42 ± 0.23
	q_0 (mg/g)	13.42 ± 0.66	7.57 ± 0.59	4.56 ± 0.55	4.22 ± 0.42
	R^2	0.873	0.721	0.675	0.638
Thomas	K_{Th} ($mL^{-1} mg^{-1} min^{-1}$)	0.07 ± 0.01	0.04 ± 0.004	0.04 ± 0.005	0.04 ± 0.006
	q_0 (mg/g)	15.16 ± 0.84	9.35 ± 0.58	6.13 ± 0.88	5.21 ± 0.43
	R^2	0.827	0.681	0.577	0.619
Yoon-Nelson	K_{YN} (min^{-1})	$0.003 \pm 3.5 \times 10^{-4}$	$0.002 \pm 2.1 \times 10^{-4}$	$0.002 \pm 2.7 \times 10^{-4}$	$0.002 \pm 3.2 \times 10^{-4}$
	T_b (min)	645.9 ± 35.8	814.9 ± 50.9	466.3 ± 66.7	752.9 ± 62.4
	R^2	0.827	0.681	0.577	0.619

4. Conclusions

In this study, the basic physical and chemical properties of biochars produced from wood, coconut shell, rice straw, and fruit shell were introduced, and the detailed adsorption characteristics of Zn on these four biochars were discussed in this study. The different types of materials led to the difference in biochar adsorption capacity, which affected the alkaline mineral content of biochar and the related pH and CEC values. The results of various batch adsorption studies showed that the equilibrium solution pH had a great effect on the maximum adsorption capacity in the pH range of 2–7. FS500, with a pH of 10.84, was considered to be the most efficient biochar in the adsorption of Zn in aqueous solution. At adsorption equilibrium, the order of Zn adsorption amount of the four biochars is FS500 > WD600 > CS550 > RS500. All these data indicated that the pseudo-second-order model is preferred for the adsorption kinetics of Zn on biochars. The fixed-bed column test data were well fitted with the Dose–Response model. The adsorption capacities of WD600, CS550, RS500, and FS500 were 24.91, 15.87, 9.25, and 46.71 mg/g, respectively. The adsorption of Zn onto FS500 and RS500 reached equilibrium within 5 min. However, it took longer for WD600 and CS550 to complete a 70% adsorption. FS500 has the potential to be applied in a PRB system for treating contaminated groundwater.

The adsorption capacity and mechanism of different biochars can provide scientific data for the application of biochars. The FT-IR spectra and SEM images of the biochars can find the functional groups and morphology of biochars. In order to further study the adsorption mechanism, the FT-IR spectra and SEM images of the biochars can be used in the later stage. It is recommended that biochar be produced from a variety of feedstocks in accordance with UKBRC's standard procedures. Therefore, relevant comparisons can be made to identify biochar suitable for contaminated groundwater and to explore its mechanism of adsorption of heavy metals.

Supplementary Materials: The following supporting information can be downloaded at: <https://www.mdpi.com/article/10.3390/w15213789/s1>, Figure S1. Speciation diagram and effect of initial solution pH on the Zn adsorption; Figure S2. The fitting of pseudo-first-order model for Zn adsorption onto CS500.

Author Contributions: Formal analysis, W.X.; funding acquisition, J.L.; writing—original draft, W.X. and J.L.; writing—review, F.W.; editing the English text of a draft, Alicia Glatfelter, from Liwen Bianji (Edanz) (<http://www.liwenbianji.cn>, accessed on 1 February 2023). All authors have read and agreed to the published version of the manuscript.

Funding: This research was funded by the Basic Science (Natural Science) Project of Higher Education Institutions of Jiangsu Province (21KJB610012), Talent Introduction Program of Nanjing Polytechnic Institute (NJPI-2021-03), and the National Natural Science Foundation of China (51978157).

Data Availability Statement: The authors confirm that the data supporting the findings of this study are available within the article [and/or its Supplementary Materials].

Conflicts of Interest: The authors declare that they have no known competing financial interest or personal relationships that could have appeared to influence the work reported in this paper.

References

1. Ministry of Ecology and Environment of the People's Republic of China (MEP). *China's Ecological Environment Status Bulletin*; Ministry of Ecology and Environment of the People's Republic of China (MEP): Beijing, China, 2017.
2. The National People's Congress of the People's Republic of China (NPC). *Law on the Prevention and Control of Soil Pollution of the People's Republic of China*; The National People's Congress of the People's Republic of China (NPC): Beijing, China, 2018.
3. The State Council of the People's Republic of China (The State Council). *Water Pollution Control Action Plan*; The State Council of the People's Republic of China (The State Council): Beijing, China, 2015.
4. Jagaba, A.H.; Kutty, S.R.; Khaw, S.G.; Lai, C.L.; Isa, M.H.; Baloo, L.; Lawal, I.M.; Abubakar, S.; Umaru, I.; Zango, Z.U. Derived hybrid biosorbent for zinc(II) removal from aqueous solution by continuous flow activated sludge system. *J. Water Process Eng.* **2020**, *34*, 101152. [[CrossRef](#)]
5. GB/T 14848-2017; General Administration of Quality Supervision, Inspection and Quarantine of the People's Republic of China. *Quality Standard for Ground Water*. Standards Press of China: Beijing, China, 2017.
6. Shek, T.H.; Ma, A.; Lee, V.K.; McKay, G. Kinetics of zinc ions removal from effluents using ion exchange resin. *Chem. Eng. J.* **2009**, *146*, 63–70. [[CrossRef](#)]
7. Abdullah, N.; Gohari, R.; Yusof, N.; Ismail, A.; Juhana, J.; Lau, W.; Matsuura, T. Polysulfone/hydrous ferric oxide ultrafiltration mixed matrix membrane: Preparation, characterization and its adsorptive removal of lead (II) from aqueous solution. *Chem. Eng. J.* **2016**, *289*, 28–37. [[CrossRef](#)]
8. Srivastava, N.K.; Majumder, C.B. Novel biofiltration methods for the treatment of heavy metals from industrial wastewater. *J. Hazard. Mater.* **2008**, *151*, 1–8. [[CrossRef](#)]
9. Matouq, M.; Jildeh, N.; Qtaishat, M.; Hindiyeh, M.; Al Syouf, M.Q. The adsorption kinetics and modeling for heavy metals removal from wastewater by Moringa pods. *J. Environ. Chem. Eng.* **2015**, *3*, 775–784. [[CrossRef](#)]
10. Chen, X.; Chen, G.; Chen, L.; Chen, Y.; Lehmann, J.; McBride, M.B.; Hay, A.G. Adsorption of copper and zinc by biochars produced from pyrolysis of hardwood and corn straw in aqueous solution. *Bioresour. Technol.* **2011**, *102*, 8877–8884. [[CrossRef](#)]
11. Li, Q.; Tang, L.; Hu, J.; Jiang, M.; Shi, X.; Zhang, T.; Li, Y.; Pan, X. Removal of toxic metals from aqueous solution by biochars derived from long-root Eichhornia crassipes. *R. Soc. Open Sci.* **2018**, *5*, 180966. [[CrossRef](#)]
12. Qian, T.T.; Wu, P.; Qin, Q.Y.; Huang, Y.N.; Wang, Y.J.; Zhou, D.M. Screening of wheat straw biochars for the remediation of soils polluted with Zn (II) and Cd (II). *J. Hazard. Mater.* **2019**, *365*, 311–317. [[CrossRef](#)] [[PubMed](#)]
13. Zhang, Y.; Jin, F.; Shen, Z.; Lynch, R.; Al-Tabbaa, A. Kinetic and equilibrium modelling of MTBE (methyl tert-butyl ether) adsorption on ZSM-5 zeolite: Batch and column studies. *J. Hazard. Mater.* **2018**, *347*, 461–469. [[CrossRef](#)] [[PubMed](#)]
14. US. EPA. *Permeable Reactive Subsurface Barriers for the Interception and Remediation of Chlorinated Hydrocarbon and Chromium (VI) Plumes in Ground Water*; EPA/600/F-97/008; U.S. Environmental Protection Agency, Office of Research and Development: Washington, DC, USA, 1997; 4p.
15. Wilkin, R.; Jim, W.; David, J. *Performance Assessment of a Permeable Reactive Barrier for Ground Water—Remediation Fifteen Years after Installation*; EPA/600/F-13/324; US EPA: Washington, DC, USA, 2013.
16. Wilkin, R.T.; Acree, S.D.; Ross, R.R.; Puls, R.W.; Lee, T.R.; Woods, L.L. Fifteen-year assessment of a permeable reactive barrier for treatment of chromate and trichloroethylene in. *Sci. Total Environ.* **2014**, *468–469*, 186–194. [[CrossRef](#)] [[PubMed](#)]
17. McGovern, T.; Guerin, T.F.; Horner, S.; Davey, B. Design, construction and operation of a funnel and gate in situ permeable reactive barrier for remediation of petroleum hydrocarbons in groundwater. *Water Air Soil Pollut.* **2002**, *136*, 11–31. [[CrossRef](#)]
18. Obiri-Nyarko, F.; Grajales-Mesa, S.J.; Malina, G. An overview of permeable reactive barriers for in situ sustainable groundwater remediation. *Chemosphere* **2014**, *111*, 243–259. [[CrossRef](#)]
19. Shen, Z.; Zhang, Y.; Jin, F.; Alessi, D.S.; Zhang, Y.; Wang, F.; Al-Tabbaa, A. Comparison of nickel adsorption on biochars produced from mixed softwood and Miscanthus straw. *Environ. Sci. Pollut. Res.* **2018**, *25*, 14626–14635. [[CrossRef](#)] [[PubMed](#)]
20. Shen, Z.; Jin, F.; Wang, F.; McMillan, O.; Al-Tabbaa, A. Sorption of lead by Salisbury biochar produced from British broadleaf hardwood. *Bioresour. Technol.* **2015**, *193*, 553–556. [[CrossRef](#)]
21. Zhang, Y.; Jin, F.; Shen, Z.; Wang, F.; Lynch, R.; Al-Tabbaa, A. Adsorption of methyl tert-butyl ether (MTBE) onto ZSM-5 zeolite: Fixed-bed column tests, breakthrough curve modelling and regeneration. *Chemosphere* **2019**, *220*, 422–431. [[CrossRef](#)]
22. Zhang, Y.; Qin, J.; Yi, Y. Biochar and hydrochar derived from freshwater sludge: Characterization and possible applications. *Sci. Total Environ.* **2021**, *763*, 144550. [[CrossRef](#)] [[PubMed](#)]
23. Kumar, S.; Loganathan, V.A.; Gupta, R.B.; Barnett, M.O. An Assessment of U(VI) removal from groundwater using biochar produced from hydrothermal carbonization. *J. Environ. Manag.* **2011**, *92*, 2504–2512. [[CrossRef](#)]

24. Gillham, R.W.; O'Hannesin, S.F. Enhanced degradation of halogenated aliphatics by zero-valent iron. *Groundwater* **1994**, *32*, 958–967. [[CrossRef](#)]
25. Beiyuan, J.; Awad, Y.M.; Beckers, F.; Tsang, D.C.; Ok, Y.S.; Rinklebe, J. Mobility and Phytoavailability of As and Pb in a contaminated soil using pine sawdust biochar under systematic change of redox conditions. *Chemosphere* **2017**, *178*, 110–118. [[CrossRef](#)]
26. Zhang, H.; Chen, C.; Gray, E.M.; Boyd, S.E. Effect of feedstock and pyrolysis temperature on properties of biochar governing end use efficacy. *Biomass Bioenergy* **2017**, *105*, 136–146. [[CrossRef](#)]
27. Ahmad, M.; Rajapaksha, A.U.; Lim, J.E.; Zhang, M.; Bolan, N.; Mohan, D.; Vithanage, M.; Lee, S.S.; Ok, Y.S. Biochar as a sorbent for contaminant management in soil and water: A review. *Chemosphere* **2014**, *99*, 19–33. [[CrossRef](#)]
28. O'Connor, D.; Peng, T.; Zhang, J.; Tsang, D.C.W.; Alessi, D.S.; Shen, Z.; Hou, D. Biochar application for the remediation of heavy metal polluted land: A review of in situ field trials. *Sci. Total Environ.* **2018**, *619*, 815–826. [[CrossRef](#)]
29. Shen, Z.; Zhang, Y.; McMillan, O.; Jin, F.; Al-Tabbaa, A. Characteristics and mechanisms of nickel adsorption on biochars produced from wheat straw pellets and rice husk. *Environ. Sci. Pollut. Res.* **2017**, *24*, 12809–12819. [[CrossRef](#)] [[PubMed](#)]
30. Tan, W.; Zhou, H.; Tang, S.; Zeng, P.; Gu, J.; Liao, B. A Enhancing Cd(II) adsorption on rice straw biochar by modification of iron and manganese oxides. *Environ. Pollut.* **2022**, *300*, 118899. [[CrossRef](#)] [[PubMed](#)]
31. GB/T 12496.7-1999; Test Methods of Wooden Activated Carbon-Determination of pH. The State Forestry Administration of the People's Republic of China: Beijing, China, 1999.
32. Gillman, G.; Sumpter, E. Modification to the compulsive exchange method for measuring exchange characteristics of soils. *Aust. J. Soil Res.* **1986**, *24*, 61. [[CrossRef](#)]
33. Cheung, C.W.; Porter, J.F.; McKay, G. Sorption kinetic analysis for the removal of cadmium ions from effluents using bone char. *Water Res.* **2001**, *35*, 605–612. [[CrossRef](#)] [[PubMed](#)]
34. Choy, K.K.H.; Ko, D.C.K.; Cheung, C.W.; Porter, J.F.; McKay, G. Film and intraparticle mass transfer during the adsorption of metal ions onto bone char. *J. Colloid Interface Sci.* **2004**, *271*, 284–295. [[CrossRef](#)]
35. Naidu, R.; Kookana, R.S.; Sumner, M.E.; Harter, R.D.; Tiller, K.G. Cadmium Sorption and Transport in Variable Charge Soils: A Review. *J. Environ. Qual.* **1997**, *26*, 602–617. [[CrossRef](#)]
36. Wang, F.; Wang, H.; Jin, F.; Al-Tabbaa, A. The performance of blended conventional and novel binders in the in-situ stabilisation/solidification of a contaminated site soil. *J. Hazard. Mater.* **2015**, *285*, 46–52. [[CrossRef](#)]
37. Wang, F.; Al-Tabbaa, A. Leachability of 17-year old stabilised/solidified contaminated site soils. In *GeoCongress 2014: Geo-Characterization and Modeling for Sustainability*; ASCE: Atlanta, GA, USA, 2014.
38. Kogbara, R.B.; Al-Tabbaa, A.; Yi, Y.; Stegemann, J.A. pH-dependent leaching behaviour and other performance properties of cement-treated mixed contaminated soil. *J. Environ. Sci.* **2012**, *24*, 1630–1638. [[CrossRef](#)]
39. Chen, T.; Zhou, Z.; Xu, S.; Wang, H.; Lu, W. Adsorption behavior comparison of trivalent and hexavalent chromium on biochar derived from municipal sludge. *Bioresour. Technol.* **2015**, *190*, 388–394. [[CrossRef](#)] [[PubMed](#)]
40. Feng, C.; Li, J.; Fang, Y.; Zhang, J. The treatment process for groundwater with excessive zinc content. *Sci. Technol. Eng.* **2021**, *21*, 11023–11033.
41. Masoumeh, F.; Adel, R.; Nosratollah, N.; Shahin, O. Kinetic and equilibrium studies on the zinc adsorption-desorption characteristics of some promising biochars in aqueous solutions. *Arab. J. Geosci.* **2022**, *15*, 794.

Disclaimer/Publisher's Note: The statements, opinions and data contained in all publications are solely those of the individual author(s) and contributor(s) and not of MDPI and/or the editor(s). MDPI and/or the editor(s) disclaim responsibility for any injury to people or property resulting from any ideas, methods, instructions or products referred to in the content.